

0040-4020(95)00452-1

Branched Oligodeoxynucleotides: Automated Synthesis and Triple Helical Hybridization Studies

Michael von Büren, Gorm V. Petersen, Kim Rasmussen, Gunda Brandenburg and Jesper Wengel*

Department of Chemistry, Odense University, DK-5230 Odense M, Denmark

Finn Kirpekar

Department of Molecular Biology, Odense University, DK-5230 Odense M, Denmark

Abstract: Automated synthesis of novel mono-branched ("Y-shaped") and double-branched ("H-shaped") oligodeoxynucleotide analogues has been accomplished by use of phosphoramidite chemistry. The synthetic strategy involves stereoselective 3'-*O*-phosphitylation of nucleoside **2** to give building block **3** and fully automated stereoselective elongation and subsequent branching of amidite **3** on a DNA-synthesizer. Thus, this strategy allows construction of branched nucleic acid molecules with sequences of arbitrary branch length and base composition. Compared to the corresponding linear analogues, the novel branched oligodeoxynucleotides exhibited increased thermal stability in intramolecular and intermolecular hybridization experiments.

INTRODUCTION

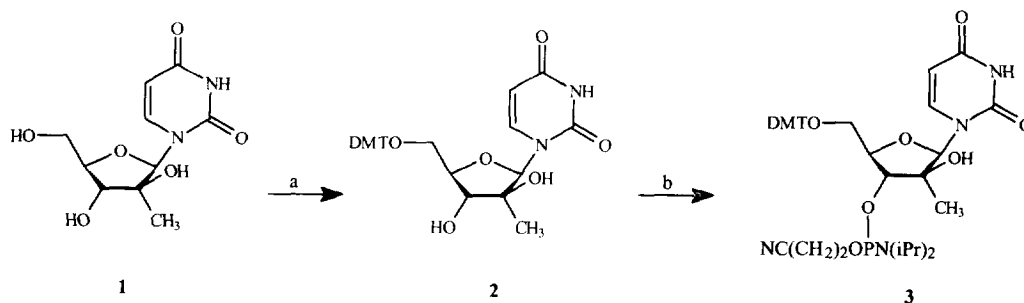
Reports on research in the field of synthetic branched nucleic acids have been few in number so far. Most of the work in this area has been focused on synthesizing, investigating and mimicking the branching moiety of lariat-RNA¹⁻⁶ occurring in eukaryotic mRNA splicing. Synthesis of branched oligonucleotides has been performed largely by use of rather laborious solution phase methods.¹⁻⁵ However, there have been accounts of solid phase synthesis as well, but they have either resulted in identical sequences in two of the three branches of the oligonucleotide^{6a,7} or involved (off-machine) cleavage of additional protective groups before branching.^{6b,8,9} Recently, we have developed a fully automated synthetic strategy for preparation of branched ("Y-shaped") oligodeoxynucleotides (ODNs) with sequences of arbitrary length and base composition.¹⁰ In the present paper, this synthetic strategy is described in full detail, and its versatility is demonstrated by synthesis of a variety of novel mono-branched ("Y-shaped") and double-branched ("H-shaped") ODN analogues. This synthetic method and the novel DNA structures may contribute to the growing interest in constructing macromolecules with a well-defined chemical composition and structure.^{7,11}

The "antisense" principle of synthesizing rationally designed drugs in the form of modified oligonucleotides to interfere with gene expression (through drug:mRNA duplex formation) has become a subject of great interest during the last years. Thus, much research is currently focused on the manifold aspects

and challenges involved in the *in vivo* applications of these molecules.¹² The targeting of single-stranded nucleic acids by bi-molecular triplex formation has previously been addressed by use of back-folding linear DNA.¹³ As an extension of this approach, we designed the sequences of the branched ODNs to allow for evaluation of the potential of these molecules in high-affinity targeting of single-stranded nucleic acids.

RESULTS AND DISCUSSION

1-(2-Methyl- β -D-arabinofuranosyl)uracil (**1**) was synthesized by known procedures in four steps from uridine.^{14,15} The obtained ¹H NMR and ¹³C NMR data for **1** were in good agreement with the published values. The configuration around C-2' was verified by a ¹H NOE experiment on **1**. Especially, the mutual key NOE contacts between 2'-C-CH₃, 1'-H and 4'-H confirmed the positioning of the 2'-C-CH₃ substituent at the α -face of the furanose ring.¹⁶ Nucleoside **1** was incorporated as branching point into oligodeoxynucleotides after transformation into the phosphoramidite synthon **3** (Scheme 1). Thus, protection of the 5'-hydroxyl function of triol **1** to give 1-(5-*O*-(4,4-dimethoxytrityl)-2-methyl- β -D-arabinofuranosyl)uracil (**2**) was achieved in 59 % yield using 4,4'-dimethoxytrityl chloride in pyridine. Subsequent regioselective phosphitylation of the secondary 3'-hydroxyl by reaction with 2-cyanoethyl *N,N*-diisopropylaminophosphoramidochloridite in dichloromethane afforded the desired amidite **3** in 91 % after precipitation from petroleum ether. According to ³¹P NMR, no trace of 2'-*O*-phosphitylated product was detected.¹⁷ This corresponds to earlier reported results of completely regioselective phosphitylations when differentiating between a primary and a tertiary hydroxyl functionality in 2'-deoxy-3'-*C*-hydroxymethyl nucleosides.^{17b,17c} Likewise, synthesis of *arabino*-oligonucleotide analogues has been reported using an unprotected *arabino*-phosphoramidite.¹⁸ In the latter case, the *secondary nature* of the unprotected 2'-hydroxyl group (as compared to the *tertiary nature* of the 2'-hydroxyl group in **2**) induced the formation of minor amounts of 2'-*O*-amidite by-products.¹⁸



Scheme 1

a) DMTCl, pyridine; b) 2-cyanoethyl *N,N*-diisopropylphosphoramidochloridite, *N,N*-diisopropylethylamine, CH₂Cl₂. DMT = 4,4'-dimethoxytrityl

All branched ODNs (Tables 1-3) reported here were synthesized by use of the fully automated strategy illustrated in Figure 1. The chemistry employed was essentially the standard phosphoramidite chemistry,¹⁹ with cycles consisting of detritylation, coupling, capping and oxidation. Changes were made in the coupling times and amidite concentrations of a number of the synthesis cycles as described below and in the experimental section.

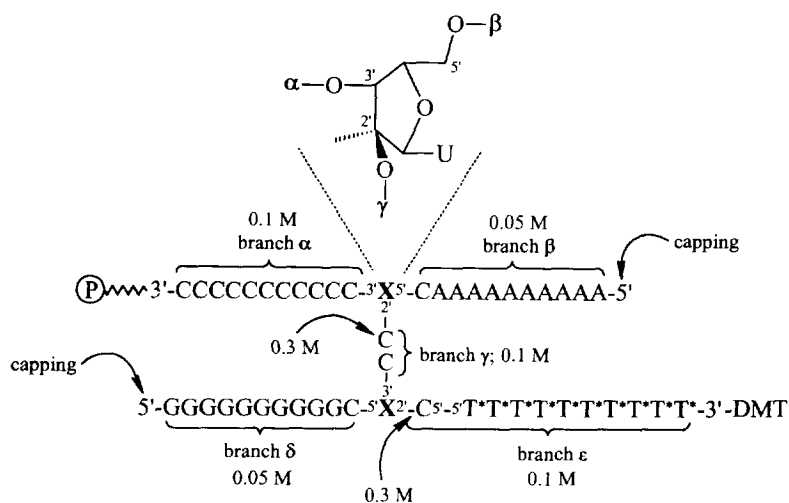


Figure 1. Synthetic strategy used to construct branched oligodeoxynucleotides and the structure around the modified uridine nucleotide derived from synthon 3 (nucleotide X). $\text{\textcircled{P}}$ is the solid support. C, A and G are the common 2'-deoxynucleotides. The branches are designated α , β , γ , δ and ϵ , representing the order of their addition to the growing molecule. The amidite concentrations used during synthesis of the various branches are indicated. Synthon 3 is used in 0.15 M concentration. The branching step is done with 0.3 M amidite concentration. "Capping" stands for the separate capping cycle employed to terminate linear chain elongation before the actual branching step. The sequence of events in the synthesis of mono-branched ("Y-shaped") ODNs (A-D, G-J and L-R) is: 1) synthesis of branch α , 2) incorporation of X, 3) synthesis of branch β , 4) capping, 5) branching and 6) synthesis of branch γ . To prepare double-branched ("H-shaped") ODNs (U, X-Z and AB-AG), the synthesis is continued in the following manner: 7) incorporation of X, 8) synthesis of branch δ , 9) capping, 10) branching and 11) synthesis of branch ϵ . T* is thymidine with reversed polarity derived from 3'-O-DMT-thymidine-5'-O-phosphoramidite. In the enlarged view of X on top, U stands for uracil-1-yl. The strategy is illustrated for a synthesized double-branched ODN containing the forty-seven nucleotides shown. The composition of this ODN was confirmed by MALDI-MS (mass calculated: 14671.53 Da; mass found: 14668.80 Da).

The ODN synthesis (Figure 1) was commenced by constructing branch α by use of standard amidite concentrations (0.1 M) and standard coupling time (2 min). The modified uridine nucleotide X was subsequently incorporated using amidite 3 in 0.15 M concentration and a coupling time of 12 min. To prevent

premature branching at the tertiary 2'-hydroxyl functionality of **X**, elongation of branch β was accomplished with 0.05 M amidite solutions (2 min couplings). When branch β was completed, a separate capping cycle, consisting of the detritylation and twofold capping parts of the regular synthesis cycles, was used to block further ODN elongation at the 5'-end. Synthesis of branch γ was initiated by branching at the tertiary 2'-hydroxyl of nucleotide **X** with triple concentrated (0.3 M) amidite solution and 12 min coupling, and subsequently continued by use of standard couplings (0.1 M concentrations, 2 min couplings), to afford "Y-shaped" ODNs. Whenever double-branching was desired ("H-shaped ODNs"), a second branching nucleotide **X** was incorporated at the end of branch γ . Branches δ and ϵ were subsequently added as described for branches β and γ , respectively. The DMT group of the last nucleotide incorporated was retained as purification aid for all modified ODNs. The strategy presented here eliminates the need of any additional protecting group and is completely automated. It exploits the chemical characteristics of the incorporated **X** containing a sterically hindered tertiary hydroxyl functionality. Thus, this hydroxyl group is neither capped during the capping step of the synthesis cycles nor is it prematurely branched when elongating the ODN in the 3'-5' direction when using the optimized half concentrated amidite solutions (branches β and ϵ). Preliminary experiments had shown, however, that use of normal amidite concentrations and longer coupling times do cause limited but unwanted branching, *e.g.* during elongation of branch β , as indicated by stepwise coupling yields slightly exceeding 100 %.

The coupling yields, as VIS-spectrometrically determined by the release of the DMT-cation during detritylation, were > 99 % for all 2 min couplings. The branching monomer **X** was incorporated in yields of typically 70-85 %. Sterical hindrance from the α -2'-*O*-methyl group of **X** may contribute to the generally lowered coupling yield when incorporating **X**. The branching step (*e.g.* incorporation of the first nucleotide in branch γ) was accomplished in 60-70 % yield. The reduced average coupling yield in this step we mainly attribute to the tertiary nature of the 2'-hydroxyl. This assumption is strongly supported by the absence of any appreciable 2'-hydroxyl capping and branching during synthesis of *e.g.* branch β .

The ODNs were cleaved off the solid support and simultaneously deprotected by incubation in concentrated aqueous ammonia at room temperature for three days. The resulting crude ODNs were purified on disposable reversed-phase cartridges. Since all modified ODNs were left with the final DMT group on, they were separated from all the truncated sequences which were capped during the syntheses and therefore lacked the DMT handle.²⁰ The masses, and therefore the compositions, of ODNs **P**, **Q**, **AA**, **AB** and **AC** as representative examples, were experimentally confirmed by MALDI-MS^{21,22} to be within 0.5 ‰ of the calculated values. MALDI-MS spectra and HPLC-profiles of mono-branched ODN **Q** and double-branched ODN **AC** are depicted in Figure 2. The peaks at 2855.81 Da and 5428.31 Da in the MALDI-MS spectra are internal PNA calibrants. The relatively large deviation (~0.5 ‰) between the calculated and measured mass of ODN **AC** and the relatively low intensity of the molecular-ion peak at 11184.50 Da can be explained by the high molecular weight of **AC**.

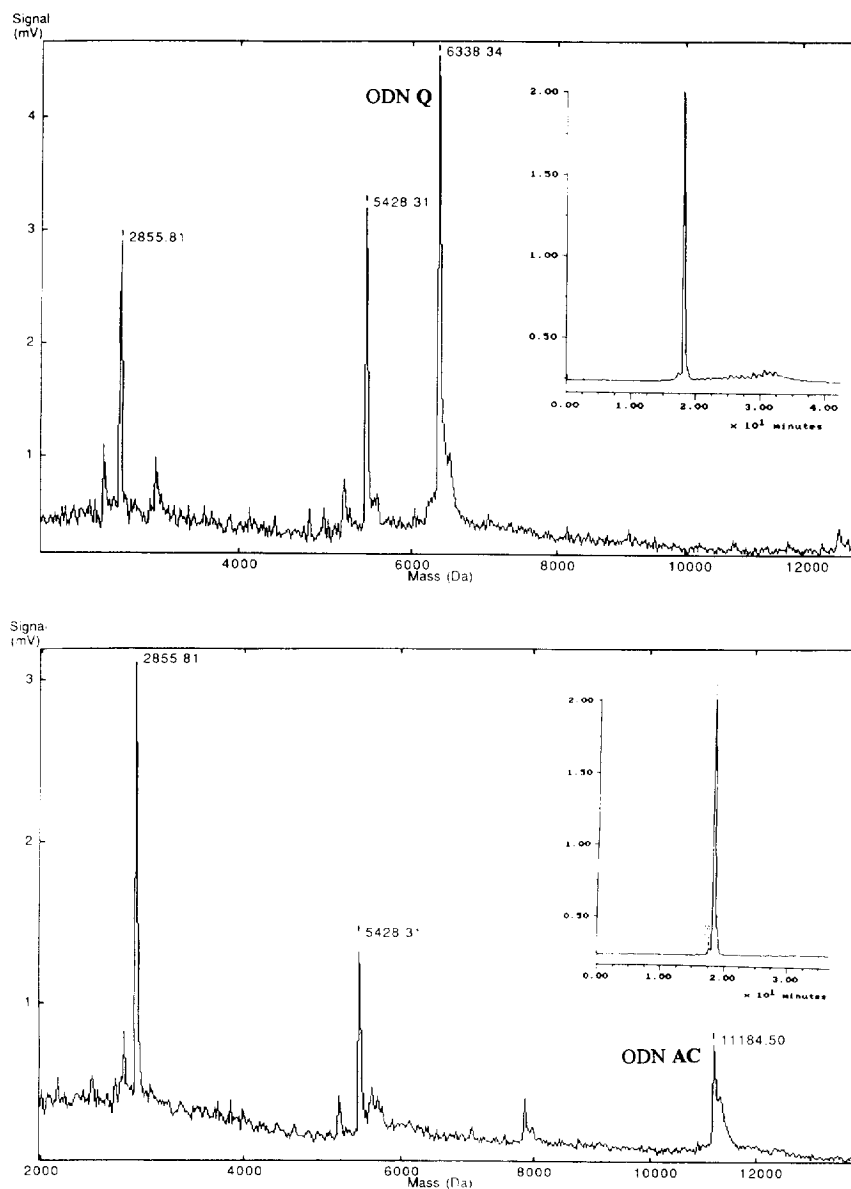


Figure 2. MLDI-MS spectra and HPLC-profiles (inserts) of mono-branched ODN Q and double-branched ODN AC

To further verify the assigned structures of the branched ODNs, the experiment outlined in Figure 3 was performed. Double-branched ODNs **AG** and **AB** were 5'-end [³²P]-labelled and subsequently digested by snake venom phosphodiesterase (SVPDE, 3'-exonuclease).²³ The digestion was followed by use of denaturing gel electrophoresis as shown in Figure 3. Digestion proceeds from the two 3'-ends (branches α and ϵ) of the two branched ODNs until the enzyme reaches the modified nucleotide **X** (branch α) and the 5'-end of a cytidine

monomer (branch ϵ). It is clear that **AG** (removal of 3 nucleotides) and **AB** (removal of 16 nucleotides) are digested to the same product (assigned as **ODN AH**, after 300 min digestion, lane b and lane d) which verifies the branched structures of the synthesized molecules.

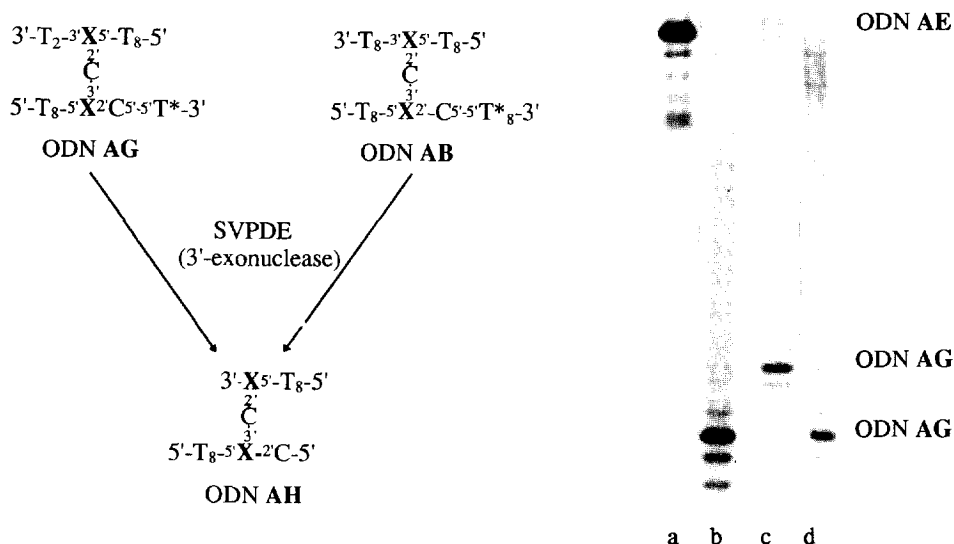


Figure 3. Snake venom phosphodiesterase (SVPDE) digestion of 32 P-labelled ODNs **AG** and **AB**. Lane a and lane c: no enzyme added; lane b and lane d: 300 min digestion. The symbols are explained in Figure 1.

The hybridization studies on the modified ODNs were carried out in medium salt buffer as described in the experimental section. All cooperative strand dissociations of double and/or triple helical nature were detected through hyperchromicity at 260 nm. Triple helix^{24,25} (T:A:T) dissociation was confirmed by observing the characteristic hyperchromic absorbance change at 284 nm,^{26,27} a wavelength where melting duplexes (A:T) do not show any hyperchromicity. The first set of ODNs (Table 1) was designed to investigate intramolecular hybridization. ODNs **A-D** all contain one dA₁₂ strand and one T₁₂ strand oriented in an antiparallel manner to each other which makes a Watson-Crick duplex formation possible. ODNs **A** and **B** additionally contain a second T₁₂ strand being antiparallel to the first T₁₂ and parallel to the dA₁₂ strand, which enables triple helix formation through association in the Hoogsteen mode to the Watson-Crick duplex in its major groove.^{24,25} ODNs **C** and **D**, on the other hand, contain a poly dC strand as third strand which excludes formation of a triple helical complex. Upon thermal denaturation, ODNs **A** and **B** both showed a bi-phasic melting profile at 260 nm, whereas ODNs **C** and **D** displayed only one melting point. The lower meltings of **A** and **B** (59 °C and 47 °C, respectively) were confirmed at 284 nm. The higher melting temperatures of **A** and **B** and the melting temperatures of **C** and **D** were all in the same range (66-67 °C) and could not be detected at 284 nm. From these results we attribute the melting at approximately 66 °C to Watson-Crick duplex dissociation of

$dA_{12}:T_{12}$, which is possible with all four molecular designs, and the lower meltings of **A** and **B** to the dissociation of the third T_{12} strand from the duplex. Considering the large difference in the lower melting temperature (12 °C) between **A** and **B**, we conclude that triple helix formation is favoured when the third strand was connected to **X** at the 2'-*O* position. The small deviations between the four duplex melting temperatures indicate no significant difference in the stability between duplexes formed from branches α and γ (Figure 1) and from α and β , both containing a five-nucleotide linker. As the unmodified reference duplex $T_{12}:dA_{12}$ melts at 36 °C, the branched ODNs **A-D** seem favourably preorganized for the formation of stable duplexes. The high triple helix melting data of branched ODNs as **A** and **B** may facilitate future experiments on structural and conformational requirements for triple helix formation. As a linear analogue of ODN **A** we synthesized **E**. The observed melting behaviour of **E** was quite distinct from that of **A**. The duplex melting at 61.5 °C we attribute to the dissociation of the T_{12} on the 3'-end from dA_{12} (five-nucleotide linker is more favourable for back-folding). The lower melting point of 23 °C originates probably from an intermolecular triple helix dissociation. Important are the differences in melting behaviour between **A** and **E**. Thus, if the branching strategy would have failed during synthesis of **A**, the linear ODN **E** would have been the outcome. Therefore, the observed differences in melting temperatures between **A** and **E** prove that their structures are different. This supports the assigned branched structure of **A**.

Table 1. Intramolecular Hybridization: Synthesized Sequences and Measured Melting Temperatures (T_m)

	Sequence ^a	$T_m / ^\circ\text{C}^b$
A ¹⁰	3'-TTTTTTTTTTTTTCC-3' X ^{5'} -CCAAAAAAAAAAAAA-5' 5'-TTTTTTTTTTTTTCC/	59.0 ^c ; 66.0 ^d
B	3'-TTTTTTTTTTTTTCC-3' X ^{5'} -CCTTTTTTTTTTTT-5' 5'-AAAAAAAAAAAAAACC/	47.0 ^c ; 66.5 ^d
C ¹⁰	3'-TTTTTTTTTTTTTCC-3' X ^{5'} -CCAAAAAAAAAAAAA-5' 5'-CCCCCCCCCCCCC/	66.0 ^d
D	3'-TTTTTTTTTTTTTCC-3' X ^{5'} -CCCCCCCCCCCCC-5' 5'-AAAAAAAAAAAAAACC/	67.0 ^d
E	3'-TTTTTTTTTTTTTCC X CCAAAAAAAAAAAAAACC'TTTTTTTTTTTT-5'	23.0 ^c ; 61.5 ^d

^a A = 2'-deoxyadenosine; C = 2'-deoxycytidine; G = 2'-deoxyguanosine; T = thymidine; T* = thymidine with reversed polarity derived from 3'-*O*-DMT-thymidine-5'-*O*-phosphoramidite; **X** = modified nucleotide derived from **3**.

^b Melting point determined as the maximum of the first derivative of the melting curve at 260 nm.

^c Transition confirmed at 284 nm.

^d No transition detectable at 284 nm.

The second set of ODNs (Table 2) was synthesized to evaluate the recognition potential of mono-branched ODNs towards single-stranded nucleic acid targets (poly-dA strands). Hybridization was to be achieved through Watson-Crick pairing of one part of the modified branched ODN with the target sequence and through subsequent Hoogsteen pairing of another part with the Watson-Crick duplex. As the 2'-hydroxyl of the branching nucleotide **X** points into the major groove of a double helix, utilisation of **X** in this context fulfils one basic requirement of successful triple helix formation: the location of the third strand in the major groove. ODNs **G-J** (Table 2) are branched derivatives of oligomer **F** with a varying number (one to four) of dC monomers between **X** and the T₇ moiety of the third branch. Upon hybridization of ODNs **G-J** with dA₁₂, melting temperatures were unchanged compared to the linear reference **F**, and no hyperchromicity at 284 nm accompanied the dissociations. These data fit the model that the second T strand has to be antiparallel to the first T strand in T:A:T triple helices.²⁵ As a consequence, no additional stabilization originating from the third strand (branch γ) was to be expected in ODNs **G-J**. ODNs **L-R**, all branched derivatives of oligomer **K**, were designed to orient the T₇-containing third strand (branch γ), antiparallel to the duplex-forming T strand (branch α). In ODNs **K-P** the length of the dC-linker is varied from zero to four. As pointed out in the literature,²⁵ triple helix formation is very sensitive towards introduction of mismatches. Therefore, to investigate the influence of the third strand (branch γ) in potential triple helix formation, we synthesized ODNs **Q** and **R**. The observed melting points for ODNs **L-P** were increased by about 4 °C as compared to the linear reference **K**. Accompanying hyperchromicities at 284 nm confirmed the involvement of triple helix dissociation in these monophasic transitions. The melting behaviour for both **Q** and **R** was identical to that observed for the linear reference **K** ($T_m = 26$ °C, no triple helix dissociation). Thus, the involvement of the third strand (branch γ) in the formation of triple helical complexes, and in the thermal stabilization of duplexes between dA₁₂ and **L-P** compared to dA₁₂ and **K**, is confirmed. The length of the dC-linker apparently has no significant influence on the triplex formation. However, the slightly larger increases observed for **L** and **M** might indicate a preference for a short linker between **X** and the T₇ moiety. ODN **S** is a linear analogue of **N** and was synthesized to evaluate its hybridization towards dA₁₂ compared to that of **N**. The measured melting temperature of 28.5 °C was raised compared to the 26 °C of **K**, but did not reach the 30 °C obtained for **N**. As in the case between ODNs **E** and **A**, there is a clear distinction in melting behaviour between a linear analogue (**S**) and the corresponding branched analogue (**N**) which supports successful branching during synthesis of the branched molecules. The lower melting point of **S** compared to **N** may be caused by a comparatively unfavourable back-folding of the triplex-forming part at the not very tightly associated end of the Watson-Crick duplex. Consequently, attachment of the third strand in the more rigid central part of the duplex, as in oligomers **L-R**, should induce the formation of entropically more favoured triple helical complexes.

With the third set of ODNs (Table 3), we wanted to investigate the possibilities of using the developed strategy to synthesize double-branched ODNs. Besides, the sequences of the branches of these "H-shaped" ODNs were designed to allow evaluation of the potential of these molecules in targeting single-stranded nucleic acids (poly-dA strands). These molecules consist of a Watson-Crick hybridizing moiety (branches α and β ,

Table 2. Synthesized Single-Branched Sequences (plus Non-Branched Reference Strands) and Measured Melting Temperatures (T_m) from Hybridization with complementary dA₁₂

	Sequence ^a	T_m / °C ^b
F ¹⁰	3'-TTT-3'X ⁵ -TTTTTTTT-5'	29.0 ^d
G	3'-TTT-3'X ⁵ -TTTTTTTT-5' 5'-TTTTTTTC	29.0 ^d
H ¹⁰	3'-TTT-3'X ⁵ -TTTTTTTT-5' 5'-TTTTTTTCC	29.0 ^d
I	3'-TTT-3'X ⁵ -TTTTTTTT-5' 5'-TTTTTTTCCC	27.5 ^d
J ¹⁰	3'-TTT-3'X ⁵ -TTTTTTTT-5' 5'-TTTTTTTCCCC	29.0 ^d
K ¹⁰	3'-TTTTTTTT-3'X ⁵ -TTT-5'	26.0 ^d
L	3'-TTTTTTTT-3'X ⁵ -TTT-5' 5'-TTTTTTTT	30.5 ^c
M	3'-TTTTTTTT-3'X ⁵ -TTT-5' 5'-TTTTTTTC	31.0 ^c
N ¹⁰	3'-TTTTTTTT-3'X ⁵ -TTT-5' 5'-TTTTTTTCC	30.0 ^c
O	3'-TTTTTTTT-3'X ⁵ -TTT-5' 5'-TTTTTTTCCC	30.0 ^c
P ¹⁰	3'-TTTTTTTT-3'X ⁵ -TTT-5' 5'-TTTTTTTCCCC	30.0 ^c
Q	3'-TTTTTTTT-3'X ⁵ -TTT-5' 5'-TTTGTTC	26.0 ^d
R	3'-TTTTTTTT-3'X ⁵ -TTT-5' 5'-TGTGTTC	26.0 ^d
S	3'-TTTTTTTT-3'X ⁵ -TTTCCTTTTTT-5'	28.5 ^c

^a A = 2'-deoxyadenosine; C = 2'-deoxycytidine; G = 2'-deoxyguanosine; T = thymidine; X = modified nucleotide derived from 3.

^b Melting point determined as the maximum of the first derivative of the melting curve at 260 nm.

^c Transition confirmed at 284 nm.

^d No transition detectable at 284 nm.

Figure 1), a linker (branch γ) and a potential Hoogsteen pairing moiety consisting of two strands connected to the second nucleotide **X** (branches δ and ϵ). Branch ϵ had to be constructed by use of reversed amidites (as described in the experimental section) in order to obtain the necessary strand polarity for triplex formation in this part of the molecules. The ODNs were designed on the basis of four T_4 (**T** and **U**), T_6 (**V-Z**) or T_8 (**AA-AF**) branches, all having the possibility of being involved in poly-dA targeting. No cooperative meltings towards dA₉ were observed for the double-branched ODN **U** or for its linear analogue **T** (T_4 **X** T_4). This was not surprising bearing in mind that the modification **X** generally induces a lowering in melting temperatures of around 10 °C²⁸ compared to the unmodified poly-T analogues. Thus, four thymidine nucleotides on each side of the modified nucleotide **X** were inadequate for formation of a stable duplex with the dA₉ target above 10 °C. For hybridization of ODN **X** with its dA₁₃ target, we observed a 2.5 °C increase in melting temperature compared to the linear reference **V**. The mono-phasic melting of **X**: dA₁₃ was (contrary to the **V**: dA₁₃ melting) confirmed to involve triple helix dissociation by observation of a hyperchromicity change at 284 nm. For both ODN **Y** and ODN **Z**, containing a longer dC-linker between the second branching nucleotide **X** and branch ϵ , and two mismatches in branch δ , respectively, the increase in melting temperature of approximately 2 °C, compared to reference **V**, was maintained and so was the existence of triple helices. The increased thermal stabilities of the dA₁₃-complexes of **X**, **Y** and **Z** we attribute to additional binding energy originating from triple helical interactions. The above results indicate that in a given complex it is only possible for one of the two branches δ and ϵ to participate in triple helix formation. We tentatively explain this by steric considerations. Thus, upon involvement of *e.g.* branch δ in a triple helix, branch ϵ is turned away from the double helix. ODN **Y**, containing a dC₅-linker in branch ϵ , was designed to eventually compensate for this steric problem, but as mentioned above no additional increase in melting temperature was observed. Probably, by use of the relatively long dC₅-linker, either additional triple helix formation is unfavourable for entropic reasons or the cooperativity in melting is lost.

In melting experiments towards dA₁₇, ODNs **AB-AF** all exhibited weakly increased thermal stability (by approximately 1 °C) compared to the linear reference **AA**. Accompanying hyperchromicities at 284 nm confirmed a contribution from triple helical complexes. Thus, whether these ODNs were synthesized with two potential triple helix forming branches (**AB**), or with only one (**AC-AE**), make no difference on the melting behaviour. Likewise, an increase in the length of the linker between the two branching **X** nucleotides from dC₁ (**AB**) to dC₃ (**AF**) has no effect. It therefore appears that also for these " T_8 -branched" ODNs, formation of one triple helix (involving *e.g.* branch δ) precludes formation of the second one for steric and entropic reasons. Furthermore, when considering the results depicted in Table 3, it appears that the effect on the melting point through triplex stabilization decreases the longer the basic branch is (T_8 vs. T_6). This effect may likewise be of entropic origin.

Table 3. Synthesized Double-Branched Sequences (plus Non-Branched Reference Strands) and Measured Melting Temperatures (T_m) from Hybridization with Complementary dA_n

	Sequence ^a	dA_n	$T_m / ^\circ C^b$
T	3'-TTTT-3'X ⁵ -TTTT-5'	dA_9	- ^c
U	3'-TTTT-3'X ² -TTTT-5'	dA_9	- ^c
	5'-TTTTTC-5'X ² -C ⁵ -5'T*T*T*T*-3'		
V	3'-TTTTTT-3'X ⁵ -TTTTTT-5'	dA_{13}	27.0 ^d
X	3'-TTTTTT-3'X ² -TTTTTT-5'	dA_{13}	29.5 ^e
	5'-TTTTTTC-5'X ² -C ⁵ -5'T*T*T*T*T*-3'		
Y	3'-TTTTTT-3'X ⁵ -TTTTTT-5'	dA_{13}	28.5 ^e
	5'-TTTTTTC-5'X ² -CCCCC ⁵ -5'T*T*T*T*T*-3'		
Z	3'-TTTTTT-3'X ⁵ -TTTTTT-5'	dA_{13}	29.0 ^e
	5'-TGTGTC-5'X ² -C ⁵ -5'T*T*T*T*T*-3'		
AA	3'-TTTTTTTT-3'X ⁵ -TTTTTTTT-5'	dA_{17}	41.0 ^d
AB	3'-TTTTTTTT-3'X ² -TTTTTTTT-5'	dA_{17}	42.0 ^e
	5'-TTTTTTTTC-5'X ² -C ⁵ -5'T*T*T*T*T*T*-3'		
AC	3'-TTTTTTTT-3'X ⁵ -TTTTTTTT-5'	dA_{17}	42.5 ^e
	5'-TTTTTTTTC-5'X ² -CTTTTTTTTT-5'		
AD	3'-TTTTTTTT-3'X ⁵ -TTTTTTTT-5'	dA_{17}	42.5 ^e
	5'-TTTTTTTTC-5'X ²		
AE	3'-TTTTTTTT-3'X ⁵ -TTTTTTTT-5'	dA_{17}	41.5 ^e
	5'-TTTGTGTC-5'X ² -C ⁵ -5'T*T*T*T*T*T*-3'		
AF	3'-TTTTTTTT-3'X ⁵ -TTTTTTTT-5'	dA_{17}	42.0 ^e
	5'-TTTTTTTTC-5'X ² -C ⁵ -5'T*T*T*T*T*T*-3'		

^a A = 2'-deoxyadenosine; C = 2'-deoxycytidine; G = 2'-deoxyguanosine; T = thymidine; T* = thymidine with reversed polarity derived from 3'-O-DMT-thymidine-5'-O-phosphoramidite; X = modified nucleotide derived from **3**.

^b Melting point determined as the maximum of the first derivative of the melting curve at 260 nm.

^c Transition confirmed at 284 nm.

^d No transition detectable at 284 nm.

^e No melting found.

CONCLUSION

The results outlined in this report can be summarized in the following points:

1. It is possible to synthesize branched ("Y-shaped" and "H-shaped") ODN analogues using branching monomers containing an unprotected tertiary hydroxyl group as branching point. The success of this strategy is based on regioselective phosphitylation and chain elongations. The branched ODNs can be synthesized with sequences of arbitrary length and base composition.
2. Increased thermal stabilities compared to linear references, due to the formation of short triple helical complexes, has been obtained with short "Y-shaped" branched ODNs. However, compared to unmodified linear ODNs, the branched analogues, containing monomer X as branching point, exhibit lowered melting temperatures.²⁸ This may be caused by disruption of the normal Watson-Crick duplex structure upon incorporation of X.
3. In melting experiments towards complementary poly-dA strands, the double-branched ("H-shaped") ODNs showed slightly higher thermal stabilities than the corresponding linear analogues. Apparently, this increased affinity originates from formation of only one out of the two possible short triple helical complexes.

The work described here demonstrates that branched ODNs can be synthesized by the fully automated procedure. Additionally, high-affinity targeting of linear nucleic acids by triple helix forming branched ODNs seems a realistic possibility. To achieve improved affinities and selectivities compared to unmodified linear analogues, synthesis of branching monomers capable of forming highly stable duplexes should be developed.

EXPERIMENTAL

The NMR spectra were obtained on a Bruker AC250 spectrometer at 250 MHz for ¹H NMR, 63 MHz for ¹³C NMR and 101 MHz for ³¹P NMR. δ -Values are reported in ppm relative to TMS as internal standard for ¹H and ¹³C NMR, and relative to 85% H₃PO₄ as external reference for ³¹P NMR.

1-(5'-O-(4,4'-Dimethoxytrityl)-2'-C-Methyl- β -D-arabinofuranosyl)uracil (2)

4,4'-Dimethoxytrityl chloride (1.32 g, 3.89 mmol) was added to a stirred solution of 1-(2'-C-methyl- β -D-arabinofuranosyl)uracil¹⁴ (1; 0.84 g, 3.25 mmol) in dry pyridine (11 mL) at room temperature under argon. After 27 h, the reaction was quenched through addition of MeOH (2 mL) and the mixture was concentrated under reduced pressure. The resulting oil was partitioned between CHCl₃ (45 mL) and H₂O (20 mL). The

separated organic phase was subsequently washed with H₂O (3 × 10 mL), dried (Na₂SO₄), and evaporated under reduced pressure. The residual gum was purified on a silica gel column (80 g, 3 cm × 21 cm) eluting with 0-7 % (v/v) MeOH in CH₂Cl₂ containing 0.5 % (v/v) pyridine. The fractions containing the desired product were pooled and concentrated to dryness yielding a pale yellow foam (1.08 g, 1.93 mmol, 59 %). R_f = 0.40 in 10 % MeOH in CH₂Cl₂ (v/v). ¹H NMR (CDCl₃): δ 1.52 (s, 3H, 2'-CH₃); 3.48-3.57 (m, 2H, 5'-H_a, 5'-H_b); 3.71 (s, 6H, 2 × OCH₃); 3.87 (d, 1H, 4'-H, J_{3',4'} = 8.4 Hz); 4.50 (d, 1H, 3'-H, J_{3',4'} = 8.3 Hz); 5.30 (d, 1H, 5-H, J_{5,6} = 8.1 Hz); 5.86 (s, 1H, 1'-H); 6.81-7.40 (m, 13 H, aryl); 8.20 (d, 1H, 6-H, J_{5,6} = 8.1 Hz); 10.24 (br s, 1H, NH). ¹³C NMR (CDCl₃): δ 19.71 (2'-CH₃); 55.23 (2 × OCH₃); 61.23 (C-5'); 73.58 (C-3'); 79.15, 80.46 (C-2', C-4'); 87.16 (CAr₃); 89.64 (C-1'); 101.82 (C-5); 113.39, 127.11, 128.05, 128.27, 130.06, 135.32, 135.60 (aryl); 141.22 (C-6); 144.04 (aryl); 151.62 (C-2); 158.65 (aryl); 164.47 (C-4). Anal. Calcd. for C₃₁H₃₂N₂O₈·2.4 H₂O: C, 61.66 %; H, 6.14 %; N, 4.64 %; Found: C, 61.57 %, H, 6.04 %; N, 4.59 %.

1-(3'-O-(2-Cyanoethoxy(diisopropylamino)phosphino)-5'-O-(4,4'-dimethoxytrityl)-2'-C-methyl-β-D-arabinofuranosyl)uracil (3)

Nucleoside **2** (0.440 g, 0.785 mmol) was coevaporated with dry acetonitrile (3 × 5 mL) and dried overnight *in vacuo*. After dissolving **2** in dry CH₂Cl₂ (2.4 mL), *N,N*-diisopropylethylamine (0.54 mL, 3.15 mmol) and 2-cyanoethyl *N,N*-diisopropylphosphoramidochloridite (0.35 mL, 1.57 mmol) were added under vigorous stirring at room temperature under argon. After 1 h, MeOH (0.35 mL) was added, and the reaction mixture was dissolved in EtOAc (12 mL) and washed with saturated aqueous solutions of NaHCO₃ (3 × 5 mL) and NaCl (3 × 5 mL). The organic phase was dried (Na₂SO₄) and evaporated under reduced pressure. The residue was dissolved in toluene (2 mL) and the product precipitated in petroleum ether (150 mL, cooled to -65 °C). The precipitate was collected by filtration, redissolved and coevaporated three times with acetonitrile (3 × 5 mL) to give a white foam (0.545 g, 0.716 mmol, 91 %). R_f = 0.53 in 10 % MeOH in CH₂Cl₂ (v/v). ³¹P NMR: δ 151.7, 152.3.

Oligonucleotide Synthesis

All oligonucleotides were produced on a Pharmacia Gene Assembler Special® synthesizer. Solid supports (0.2 μmol scale) were obtained from Pharmacia. The regular amidites were purchased from Cruachem; the reversed thymidine-5'-phosphoramidite from Glen Research. The amidite solution volume applied for all amidite concentrations and couplings was 75 μL. The commercial amidites were used in 0.1 M concentration i) for the oligonucleotide parts synthesized before the modified nucleotide **X** was incorporated (Figure 1: branch α), and ii) after **X** was branched at the tertiary 2'-OH (branches γ and ε) and iii) for the unmodified reference and "sense" strands. Whenever a "free" 2'-OH on **X** was present (branches β and δ), oligonucleotide elongation was performed at 0.05 M amidite concentrations. For both 0.1 M and 0.05 M amidite concentrations, the coupling time employed was 2 min. The modified uridine building block **3** was used in 0.15 M concentration and the coupling time was extended to 12 min. The branching step was performed with

a 0.3 M amidite solution with 12 min coupling time. Coupling yields as determined VIS-spectrometrically were > 99 % for the synthesis cycles with 2 min coupling (with both 0.1 M and 0.05 M amidite concentrations), whereas nucleotide **X** was incorporated in yields of 70-85 %. The branching step was performed with an efficiency of 60-70 %. All synthesis cycles with the aim of chain elongation included detritylation, coupling (with variable time, as described above), capping and oxidation. The special capping cycle, which was employed before branching to terminate linear chain growth, consisted of the detritylation step and two capping steps of the regular synthesis cycles. The DMT group of the last incorporated nucleotide was left on as purification aid in the case of modified oligonucleotides and cleaved off the unmodified reference and target sequences. The oligonucleotides were deprotected and cleaved off the solid support by incubation in 32 % aqueous NH₃ at room temperature (72 h). Purification of the synthesized ODNs were achieved by use of disposable reversed-phase columns (COPTM-columns from Cruachem; procedure includes detritylation) for molecules with DMT left on, and through size exclusion chromatography (NAPTM-10-columns, Sephadex® G-25 medium from Pharmacia) for the unmodified oligonucleotides. Both procedures were carried out according to manufacturers protocols. The oligonucleotides were obtained by evaporation to dryness (Hetovac VR1 centrifuge) and quantitated in ddH₂O solution through UV extinction at 260 nm. The masses of oligonucleotides **P**, **Q**, **AA**, **AB** and **AC** were experimentally confirmed by matrix-assisted laser desorption/ionization mass spectrometry (MALDI MS)^{21,22} on a Bruker Reflex mass spectrometer. 3-Hydroxypicolinic acid was used as matrix. PNA-standards of 2855.81 Da and 5428.31 Da were added to the samples for calibration. The observed masses were all within 0.5 % of the calculated values.

Melting Point Determination

All melting point samples were 2.5 µM in each participating oligonucleotide in a 10 mM Tris-HCl pH 7 (at 25 °C), 10 mM MgCl₂, 100 mM NaCl buffer solution. The mixtures were heated to 80 °C for 10 min, allowed to cool down to room temperature for 30 min, and kept at 0-5 °C for at least 1 h prior to measurement. The melting curves were acquired on a Perkin-Elmer Lambda 2 UV/VIS spectrometer equipped with a temperature controlling system (consisting of a Peltier Temperature Programmer PTP-6 and a Heto constant temperature cooling cycle). Absorption at 260 nm and 284 nm was measured while the temperature was raised from 10 to 80 °C with a linear rise of 1 °C min⁻¹. The melting points were determined, using the PECSS software provided by Perkin-Elmer, as the maximum of the first derivative of the melting curve.

ACKNOWLEDGMENTS

Financial support from The Danish Natural Science Research Council and The Carlsberg Foundation is gratefully acknowledged.

REFERENCES AND NOTES

1. Kierzek, R.; Kopp, D. W.; Edmonds, M.; Caruthers, M. H. *Nucleic Acid Res.* **1986**, *14*, 4751.
2. Fourrey, J. L.; Varenne, J.; Fontaine, C.; Guittet, E.; Yang, Z. W. *Tetrahedron Lett.* **1987**, *28*, 1769.
3. Huss, S.; Gosselin, G.; Imbach, J.-L. *J. Org. Chem.* **1988**, *53*, 499.
4. Sekine, M.; Heikkilä, J.; Hata, T. *Bull. Chem. Soc. Jpn.* **1991**, *64*, 588.
5. Rouse, B.; Puri, N.; Viswanadham, G.; Agback, P.; Glemarec, C.; Sandström A.; Sund, C.; Chattopadhyaya, J. *Tetrahedron* **1994**, *50*, 1777.
6. a) Sproat, B. S.; Beijer, B.; Grøtli, M.; Ryder, U.; Morand, K. L.; Lamond, A. I. *J. Chem. Soc. Perkin Trans. 1* **1994**, 419. b) Grøtli, M.; Sproat, B. S. *J. Chem. Soc. Chem. Commun.* **1995**, 495.
7. Hudson, R. H. E.; Damha, M. J. *J. Am. Chem. Soc.* **1993**, *115*, 2119.
8. Azhayev, A.; Gouzaev, A.; Hovinen, J.; Azhayeva, E.; Lönnberg, H. *Tetrahedron Lett.* **1993**, *34*, 6435.
9. Dolinnaya, N.; Gryaznov, S.; Ahle, D.; Chang, C.-A.; Shabarova, Z. A.; Urdea, M. S.; Horn, T. *Biomed. Chem. Lett.* **1994**, *4*, 1011.
10. Preliminary report: Brandenburg, G.; Petersen, G. V.; Rasmussen, K.; Wengel, J. *Biomed. Chem. Lett.* **1995**, *5*, 791.
11. Zhang, Y.; Seeman, N. C. *J. Am. Chem. Soc.* **1992**, *114*, 2656.
12. Wagner, R. W. *Nature* **1994**, *372*, 333.
13. Giovannangeli, C.; Montenay-Garestier, T.; Rougée, M.; Chassignol, M.; Thuong, N. T.; Hélène, C. *J. Am. Chem. Soc.* **1991**, *113*, 7775.
14. Hayakawa, H.; Tanaka, H.; Itoh, N.; Nakajima, M.; Miyasaka, T.; Yamaguchi, K.; Iitaka, Y. *Chem. Pharm. Bull.* **1987**, *35*, 2605.
15. Matsuda, A.; Itoh, H.; Takenuki, K.; Sasaki, T.; Ueda, T. *Chem. Pharm. Bull.* **1988**, *36*, 945.
16. NOE effects: (a) irradiation of 1'-H gave effect in 2'-C-CH₃ (1.1 %) and in 4'-H (1.1 %); (b) irradiation of 2'-C-CH₃ gave effect in 1'-H (9.9 %) and in 4'-H (6.8 %); (c) irradiation of 4'-H gave effect in 1'-H (1.8 %) and in 2'-C-CH₃ (1.2 %).
17. ³¹P NMR resonances for tertiary 2-cyanoethyl *N,N*-diisopropylaminophosphoramidites are shifted upfield (5-10 ppm) compared to analogous secondary phosphoramidites. a) Tarköy, M.; Bolli, M.; Leumann, C. *Helv. Chim. Acta* **1994**, *77*, 716. b) Jørgensen, P. N.; Svendsen, M. L.; Scheuer-Larsen, C.; Wengel, J. *Tetrahedron* **1995**, *51*, 2155. c) Wengel, J.; Svendsen, M. L.; Jørgensen, P. N.; Nielsen, C. *Nucleosides Nucleotides* **1995** in press.
18. Damha, M. J.; Usman, N.; Ogilvie, K. K. *Tetrahedron Lett.* **1987**, *28*, 1633.
19. Caruthers, M. H. *Science* **1985**, *230*, 281.
20. The purity of all branched ODNs was examined by reversed phase HPLC. All purified mono-branched ODNs (A-D, G-J and L-R) displayed only one sharp peak eluting after approximately 19 min. The

purified double-branched ODNs (**U**, **X-Z** and **AB-AG**) all displayed one dominant peak eluting after approximately 19 min. Besides, impurities integrating to 2-10 % were detected. For conditions of HPLC experiments, see ref. 17b.

21. Kirpekar, F.; Nordhoff, E.; Kristiansen, K.; Roepstorff, P.; Lezius, A.; Hahner, S.; Karas, M.; Hillenkamp, F. *Nucleic Acids Res.* **1994**, *22*, 3866.
22. Svendsen, M. L.; Wengel, J.; Dahl, O.; Kirpekar, F.; Roepstorff, P. *Tetrahedron* **1993**, *49*, 11341.
23. For details of labelling and denaturing gel electrophoresis procedures, see: Nielsen, P.; Kirpekar, F.; Wengel, J. *Nucleic Acids Res.* **1994**, *22*, 703.
24. Felsenfeld, G.; Davies, D. R.; Rich, A. *J. Am. Chem. Soc.* **1957**, *79*, 2023.
25. Moser, H. E.; Dervan, P. B. *Science* **1987**, *238*, 645.
26. Pilch, D. S.; Levenson, C.; Shafer, R. H. *Proc. Natl. Acad. Sci. USA* **1990**, *87*, 1942.
27. Pilch, D. S.; Brousseau, R.; Shafer, R. H. *Nucleic Acids Res.* **1990**, *18*, 5743.
28. Melting points recorded under the conditions described in the experimental part for unmodified duplexes: dA₉:T₉ = 20.0 °C; dA₁₂:T₁₂ = 36.0 °C; dA₁₃:T₁₃ = 39.5 °C; dA₁₇:T₁₇ = 49.0 °C.

(Received in UK 9 May 1995; accepted 9 June 1995)